Journal of Oceanology and Limnology
Vol. 36 No. 5, P. 1537-1555, 2018
https://doi.org/10.1007/s00343-018-7028-6

Recent sedimentary records in the East China Sea inner shelf and their response to environmental change and human activities*

ZHANG Kaidi (张凯棣)[1, 3], LI Anchun (李安春)[1, 2, **], ZHANG Jin (张晋)[1, 3],
LU Jian (卢健)[1], WANG Hongli (王红莉)[1]

[1] *Key Laboratory of Marine Geology and Environment*, *Institute of Oceanology*, *Chinese Academy of Sciences*, *Qingdao 266071*, *China*
[2] *Laboratory for Marine Geology*, *Qingdao National Laboratory for Marine Science and Technology*, *Qingdao 266061*, *China*
[3] *University of Chinese Academy of Sciences*, *Beijing 100049*, *China*

Received Feb. 16, 2017; accepted in principle Apr. 21, 2017; accepted for publication Jul. 21, 2017

Abstract The East China Sea continental shelf is a unique area for the study of land-sea interactions and paleoenvironmental change because it receives a large amount of terrestrial material inputs. In recent decades, human activities and global climate change have greatly affected river discharges into the sea. However, changes in the deposition process caused by these factors in the East China Sea continental shelf are unclear. We collected eight short sediment cores from the East China Sea inner shelf (ECSIS) using a box core sampler in 2012 and 2015. The grainsize, ^{210}Pb, and ^{137}Cs of these cores were analyzed in order to reconstruct the deposition history since the 1950s, and to reveal human activity and climate change influences on sediment deposition in the ECSIS. Results indicated that sediment grain size became finer after 1969, turned coarser after 1987, and then further coarser since 2003, corresponding well to the three steps of sediment load drop in the Changjiang (Yangtze) River, which are mainly caused by human activities (particularly the closure of the Three Gorges Dam). Simultaneously, the East Asian Monsoon influenced the deposition process in the ECSIS by changing the intensity of coastal currents. Mean grain size variations in the fine-grained population (divided by grain size vs. standard deviation method) coincided with that of the East Asian Winter Monsoon strength and reflected its weakness in 1987. Abrupt changes in sediment grain size over a short time scale in these sediment cores were generally caused by floods and typhoons. Spectral analyses of the sediment cores showed periodicities of 10–11 and 20–22 years, corresponding to the periodicity of solar activity (Schwabe cycle and Hale cycle). Mean grain size time series also displayed a 3–8 year periodicity corresponding to El Niño Southern Oscillation periodic change.

Keyword: East China Sea inner shelf; grain size; sedimentary records; human activities; environmental change

1 INTRODUCTION

The Changjiang (Yangtze) River discharges a large amount of terrigenous sediment into the world's widest continental shelf—the East China Sea shelf forms a distinct mud deposit along the entire inner shelf. The East China Sea inner shelf (ECSIS) mud wedge extends approximately 1 000 km from the Changjiang River mouth southward into the Taiwan Strait (Xu et al., 2012), and has continuous and high-resolution records of environmental deposition. It contains a wealth of information reflecting the impact of global climate change and human activities on river systems and deposition processes. Studies on the deposition processes of this mud wedge started in the early 1980s. DeMaster et al. (1985) obtained the first deposition rates, sedimentary structure, and bioturbation data in this area. Liu et al. (2006, 2007)

* Supported by the National Natural Science Foundation of China (No. 41430965) and the Open Fund of the Key Laboratory of Marine Geology and Environment, Chinese Academy of Sciences (No. MGE2015KG08)
** Corresponding author: acli@qdio.ac.cn

documented the extension range and the two depocenters (northern: on the modern Changjiang River delta; southern: at ~27.5°N) of the mud wedge based on seismic profiles. Using seismic profiles and sediment cores, Xu et al. (2012) discussed the development history of the mud wedge and divided it into four distinct units (late-Pleistocene, 30–11 ka BP, 11–2 ka BP, and 2–0 ka BP) according to the sequence stratigraphy. Millennial-scale climate changes recorded in the sediment cores have also been revealed in previous studies (Xiao et al., 2006; Xu et al., 2009a; Liu et al., 2011). This established a sedimentary sequence throughout the Holocene, increasing our understanding of the relationship between the depositional processes and the evolution of East Asian monsoon (EAM). Simultaneously, advances have been made in the field of high resolution sedimentary records on a century scale that can reflect anthropogenic effects on ECSIS sediment diffusion, burial, and circulation (Lim et al., 2007; Liu et al., 2010; Liu and Fan, 2011; Zhao et al., 2017).

In recent decades, human activities (especially dam constructions and irrigation networking) have led to dramatic reductions in sediment discharge from many rivers globally (Carriquiry and Sánchez, 1999; Vörösmarty et al., 2003b; Walling, 2006; Milliman et al., 2008; Xu et al., 2010; Wang et al., 2011; Gupta et al., 2012). Meanwhile, spatiotemporal patterns of precipitation have been altered by the accelerating global hydrological cycle caused by global climate change, resulting in increased occurrences of extreme floods and storms in many regions (Easterling et al., 2000; Allen and Ingram, 2002; Labat et al., 2004; Restrepo et al., 2014). Both climatic and anthropogenic changes have contributed to variations in river water discharge and sediment load into the sea, and have consequently become a relevant topic on a global scale (Syvitski and Milliman, 2007; Milliman et al., 2008; Yang et al., 2015). Based on the study of sediment grain size, mineralogy, and geochemistry, it is widely believed that the contribution of the Changjiang River to the muddy depositional wedge is predominant (Xiao et al., 2006; Xu et al., 2009b, 2012). The main material supplier of this mud wedge, the Changjiang River, has a watershed population of 450 million within a drainage area of 1.8 million km^2, and it discharged 900 km^3/a water with 500 Mt/a sediment flux before its decline in the 1970s (Yang et al., 2005; Milliman and Farnsworth, 2011). In recent years, however, more than 50 000 dams have been constructed throughout the Changjiang River watershed, including the world's largest hydropower station, the Three Gorges Dam (TGD) (Xu et al., 2006; Yang et al., 2007, 2011, 2014; Xu et al., 2008).

Furthermore, the frequency of global EI Niño/Southern Oscillation (ENSO) events has increased since global climate conditions began changing during the 2000s (Liu et al., 2012). Correspondingly, river sediment loads have dramatically decreased due to human activities (especially dam construction) and climatic changes (Vörösmarty et al., 2003a, b; Xu et al., 2006; Zhang et al., 2008; Li et al., 2011). Yang et al. (2015) reported that the Changjiang River sediment discharge significantly decreased to 46.5×10^6 t/a between 1953 and 2010. Human impacts also have been reflected in the ECSIS and river delta sediments (Milliman, 1997). Magnetic susceptibility in ECSIS sediments has significantly increased from 1.8 ka due to human activities (Xu et al., 2011). Elements such as S and As in the Changjiang River subaqueous delta have increased since 1945 corresponding well with China's economic growth period (Liu and Fan, 2011).

In addition to changes in river sediment loads, climatic changes also affect the hydrodynamic environment of the ECSIS. China's climate is greatly influenced by the EAM because it transfers enormous amounts of heat and moisture between the Eurasian continent and the adjacent ocean (Zhang and Lin, 1992; Wang, 2009). Simultaneously, changes in the EAM on a centennial-to decadal-scale are controlled by variations in solar irradiance via changes in oceanic-atmospheric circulation pattern (Xiao et al., 2006; Zhou et al., 2014). The enhancement of the East Asian Winter Monsoon (EAWM) leads to the strengthening of the coastal current, resulting in an increase in sediment grain size both in the central Yellow Sea mud and ECSIS mud (Xiao et al., 2006; Hu et al., 2012; Zhou et al., 2014).

Previous studies of the ECSIS focused on millennium-scale deposition process changes. Century-scales studies are very scarce and mostly confined to estuarine areas (Lim et al., 2007; Liu et al., 2010; Liu and Fan, 2011; Zhao et al., 2017). The influence of anthropogenic activity on mud deposits, especially construction of the TGD, is unclear. Therefore, in this study, eight short sediment cores from the northern and southern inner shelf were analyzed to study changes in the deposition process of the ECSIS over recent decades, and to attempt to reveal the effects of climate change and human activity. High-resolution analysis can better reflect sedimentary changes in the short-term.

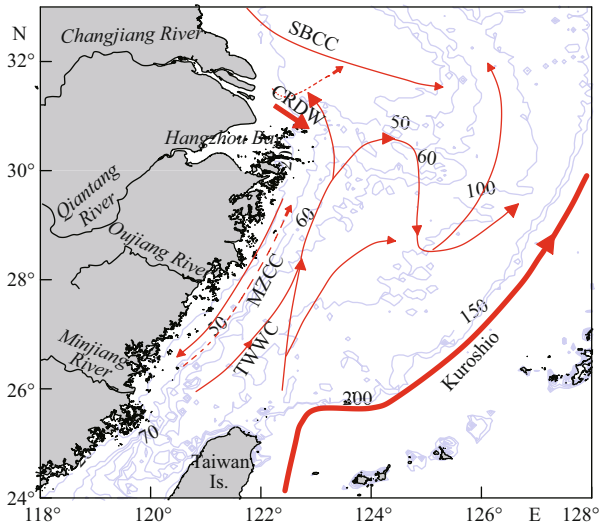

Fig.1 Currents in the East China Sea

CRDW indicates the Changjiang River Diluted Water; ZFCC indicates the Zhejiang-Fujian Coastal Current; TWWC indicates the Taiwan Warm Current; SBCC indicates the Subei Coastal Current (dotted lines are CRDW and ZFCC in summer) (modified from Liu et al., 2015).

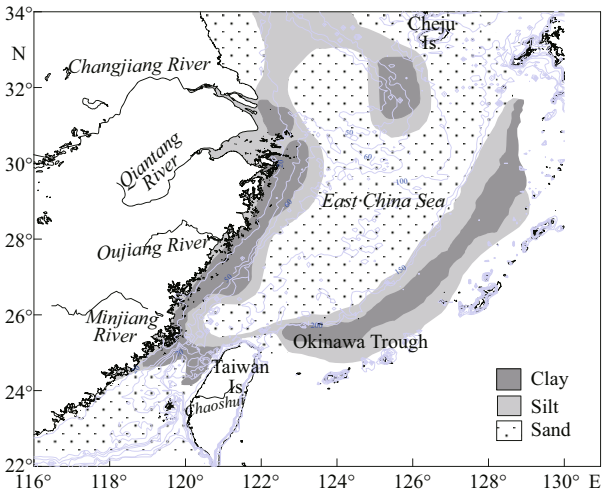

Fig.2 Surficial sediment types in the East China Sea

There are three major mud deposits: inner shelf, southwest of Cheju Island, and deeper Okinawa Trough; blue solid lines are the isobaths (modified from Xu et al., 2012).

2 STUDY AREA

The East China Sea is controlled by the northward-flowing Kuroshio Current, which flows along the shelf break, the northward Taiwan Warm Current (TWWC), the Changjiang River Diluted Water (CRDW), and the Zhejiang-Fujian Coastal Current (ZFCC) (Fig.1). Three distinct mud deposits have been formed in the East China Sea: a mud belt on the inner shelf, a mud patch southwest of Cheju Island, and a deeper deposit in the Okinawa Trough, while most of the ESC floor is covered by sand (Fig.2) (Liu et al., 2006; Xu et al., 2009a, b, 2012). Terrigenous materials on the ECSIS are mainly derived from the Changjiang River and other major local rivers, such as the Qiantang River, the Minjiang River, and the Oujiang River (Liu et al., 2007). However, these small rivers have relatively seldom sediment discharge of which the total annual sediment load is approximately 8 Mt/a, far less than the amount of sediment transported by the Changjiang River (Li, 2008). Therefore, in the present research, the impact of these small rivers was not considered. In summer months, TWWC intensifies, and the CRDW and ZFCC flow northward under the prevailing southeast monsoon, resulting in large amounts of Changjiang River discharges becoming trapped in the estuarine region. In winter, due to the strengthening northwest monsoon, the ZFCC turns southward carrying the CRDW and sediment discharge southward along the inner shelf. Most of the southward dispersed sediments are constrained on the inner shelf by the TWWC forming the inner shelf mud wedge (Guo et al., 2003; Liu et al., 2007).

Both Yuan et al. (2005, 2008, 2010a, b) and He et al. (2010) found that there are distinct cross-shelf penetrating fronts (CPFs) in the East China Sea through satellite sea-surface temperature, ocean color, and chlorophyll-*a* concentration observations. There were over 40 CPFs with penetrating distances exceeding 100 km over the East China Sea during 1998–2007 (He et al., 2010). Each CPF event lasts for few days to a month while the time scales of cross-shelf transport and surface-to-subsurface descending of the suspended sediments are a few weeks (Yuan et al., 2008; He et al., 2010). These CPFs have induced cross-shelf sediment transport over the ECSCS.

3 MATERIAL AND METHOD

Eight short sediment cores were collected in 2012 and 2015 on the ECSIS using a box core sampler (Fig.3). For improved comparison, we selected two cores from a depth of 50 m and four cores from 60 m. Subsamples were taken at 0.5 cm intervals for grain size analysis, and 2 cm intervals for ^{210}Pb and ^{137}Cs analysis.

In order to extract terrigenous materials for grain size analysis, organic matter and carbonate in bulk samples were carefully removed using 15% H_2O_2 (60 min) and 10% CH_3COOH (60 min) in a water bath at 60°C. Following this, the treated samples were soaked in 20 mL distilled water and dispersed with an ultrasonic oscillator. Grain size measurements of the

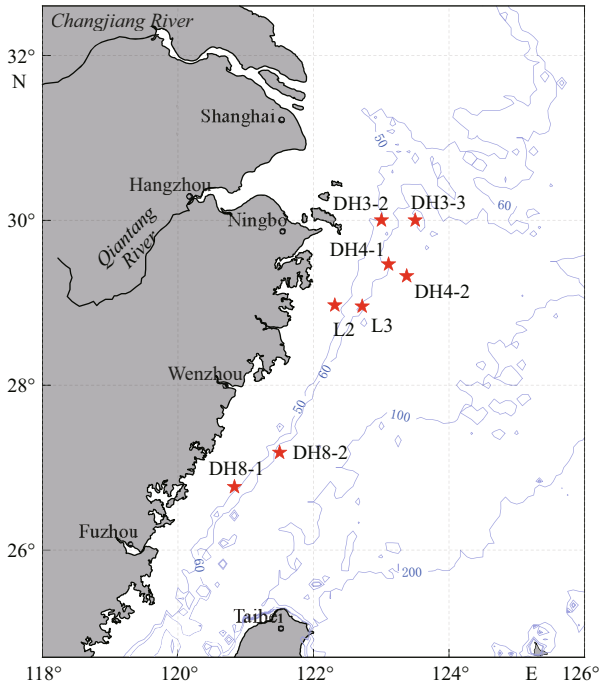

Fig.3 Study area and sampling stations

extracted terrigenous materials were performed on a Cilas 1190L Particle Size Analyzer in the Key Laboratory of Marine Geology and Environment, Institute of Oceanology, Chinese Academy of Sciences. This instrument can be used for grain size analysis in range from 0.04 to 2 500 μm and the error for repeat measurement is less than 2%. Due to the requirements of the experimental apparatus, approximately 300 mg samples were used for grain size analysis. Particle parameters were calculated with the value method according to McManus (1988).

Sediment chronology was determined using ^{210}Pb and ^{137}Cs dating methods. ^{137}Cs and ^{210}Pb were measured using an HPGe gamma-ray spectrometer at the Lake Sediment and Environment Laboratory in Nanjing Geography and Lake Institute, CAS. The standard samples of ^{137}Cs and ^{226}Ra were provided by the China Institute of Atomic Energy, and the comparative study of the ^{210}Pb standard samples was performed at the University of Liverpool, UK.

To improve our understanding of the sedimentary process, sensitive particle size components of sediment cores were separated by the method of "grain size vs. standard deviation" as selected in numerous previous studies (Boulay et al., 2003; Sun et al., 2003; Xiang et al., 2005; Xiao and Li, 2005). In addition, the time series of sample mean grain size was determined in a spectral analysis. The analysis software used was REDIFT, which is widely used in

Table 1 Sediment core information

Sample code	Water depth (m)	Length (cm)	Longitude (°E)	Latitude (°N)	Sedimentation rate (cm/a)
DH3-2	52	25	123.00	30.00	0.51
DH3-3	59	33	123.50	30.00	0.43
DH4-1	61	31.5	123.11	29.47	0.56
DH4-2	70.6	38	123.38	29.32	0.52
L2	35	36	122.31	28.97	0.47
L3	60	30.5	122.72	28.96	0.74
DH8-1	51	41	120.83	26.77	0.96
DH8-2	61	45	121.50	27.18	0.76

power spectrum analysis of unevenly spaced time series. The following parameters were used in the analysis: n50=4 (WOSA segment: Welch-Overlap-Segment-Averaging procedure) and iWin=2 (Welch spectrum window), with the remaining parameters comprising software default parameters. The parameters and their specific meanings have been previously reported by Schulz and Mudelsee (2002).

The Siberian High index and East Asian Winter Monsoon dataset are available from the National Climate Center, China Meteorological Administration (http://cmdp.ncc.cma.gov.cn/cn/index.htm). Strong breeze data from Shengsi Island are also available online: http://en.tutiempo.net/.

4 RESULT

4.1 Accumulation rates

Sedimentation rates in the sediment cores were determined using ^{210}Pb and ^{137}Cs geochronology. The ^{137}Cs level of core DH8-1 had one obvious peak corresponding to 1986 (the Chernobyl nuclear accident) (Liu and Fan, 2011). Based on the dated peak, the average deposition rate of core DH8-1 was 0.83 cm/a. Through the linear fitting of excess ^{210}Pb with depth, the average accumulation rate of core DH8-1 was 0.96 cm/a with a correlation coefficient of 0.86 cm/a (Fig.4). The deposition rates obtained by the two methods were relatively similar, indicating that the activities of excess ^{210}Pb were applicable in this study.

The deposition rate increased from north to south along the isobaths (Table 1). Sediment cores at 50 m water depth had higher deposition rates than at 60 m on similar latitude. Cores DH3-3, DH4-2 and L2 that were located near the edge area of the mud wedge had much lower accumulation rates, less than 0.5 cm/a.

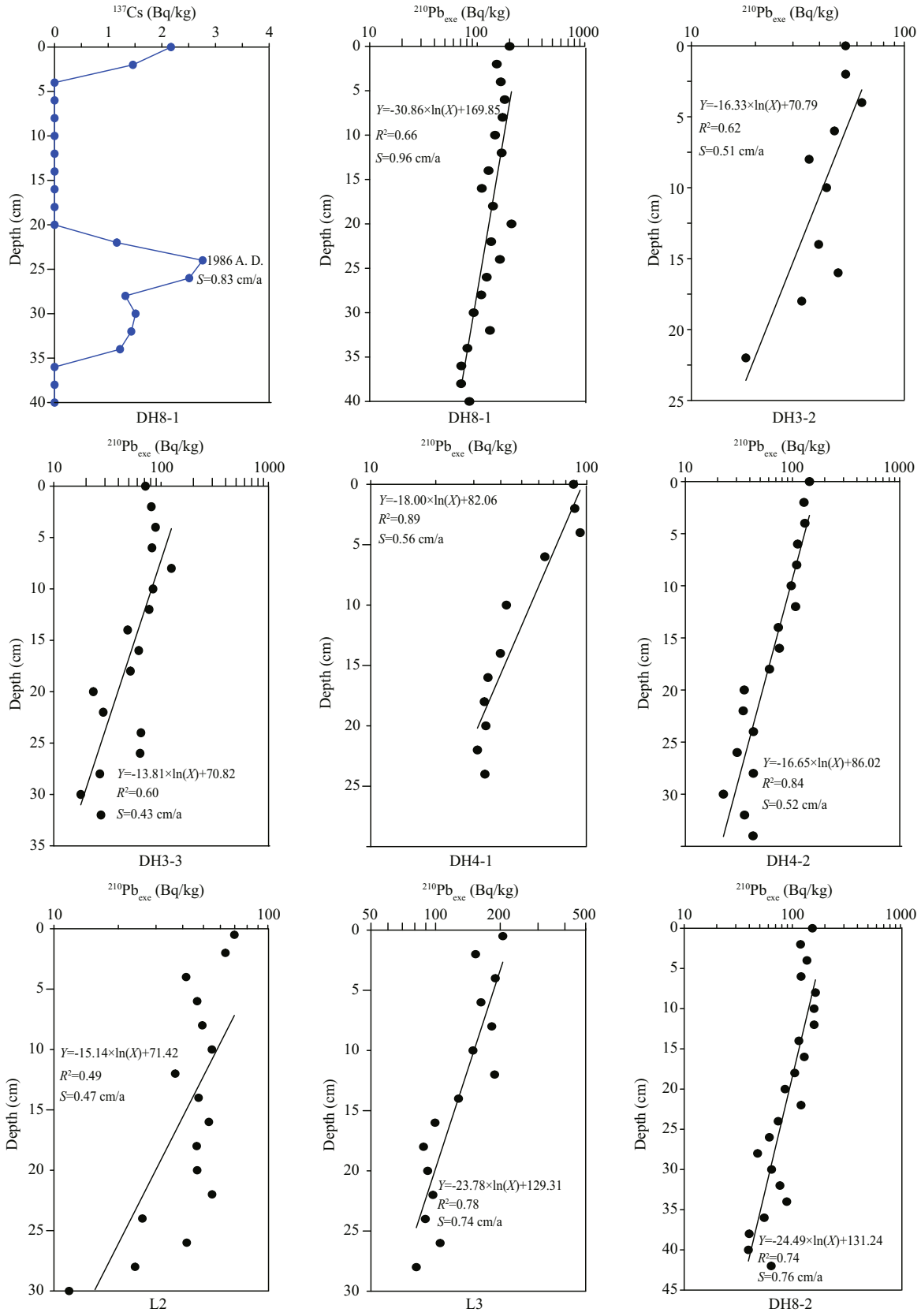

Fig.4 Excess ^{210}Pb and ^{137}Cs activities profiles of eight sediment cores

Sediment accumulation rate (S) is determined from the slope of excess ^{210}Pb activity profiles.

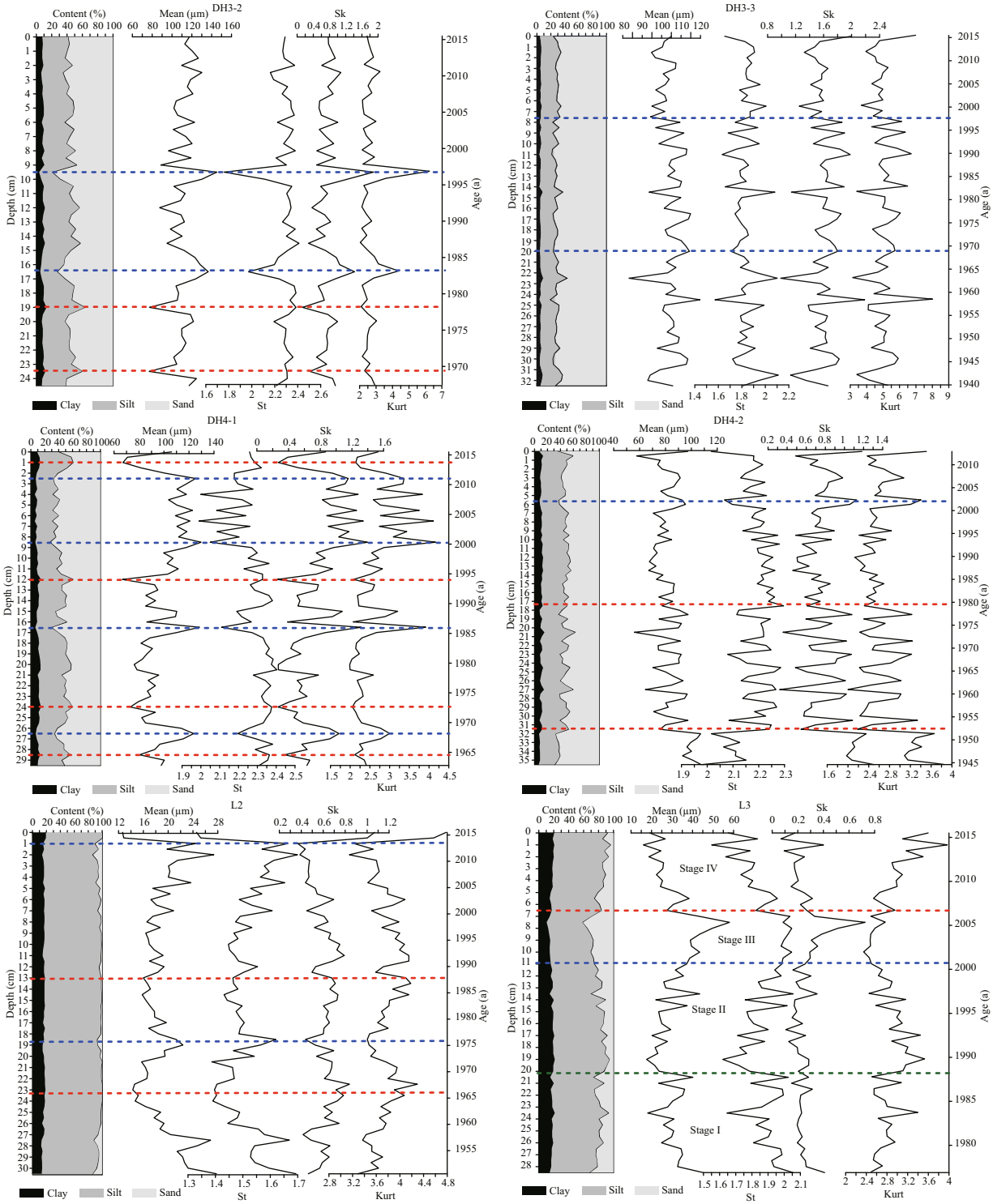

Fig.5 Grain size parameter variations of sediment cores from northern continental shelf

4.2 Grain size analysis

4.2.1 Sediment cores from the northern continental shelf

Six sediment cores were collected in the north of 29°N (Fig.3). They showed different changes over short time scales. In general, sediment grains became finer from north to south, and coarser from west to east. Sediments in cores DH3-2, DH3-3, DH4-1, and DH4-2 were coarse and dominated by sand, while the other two cores (L2 and L3) mainly comprised silt.

Cores DH3-2 and DH3-3 were located outside Hangzhou Bay. With the exception of a couple of layers, grain size only showed minor change in these two cores (Fig.5). In core DH3-2, mean grain size

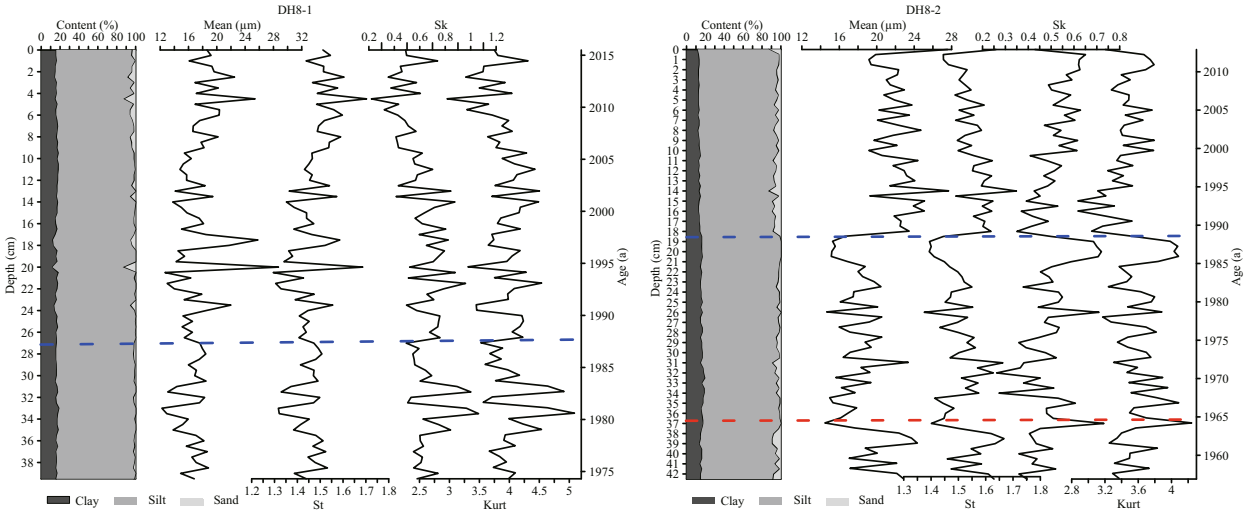

Fig.6 Grain size parameter variations among sediment cores from the southern continental shelf

coarsen upwards. Silt and clay abruptly increased in 1969 and 1979, whereas sand content suddenly increased in 1984 and 1997. The sorting and skewness changed little, and mutations occurred in some layers. Grain size parameters fluctuated acutely. Core DH3-3 was located to the east of DH3-2, and the sediment primarily comprised sand. The grain size showed a slightly fining trend since 1969. In the upper 8 cm, sediments were significantly finer and the sorting was improved, thereby signaling a new stage of deposition in 1997.

Core DH4-1 mainly comprised sand (mean: 55.67%) and silt (mean: 34.22%) with a relatively low clay content (mean: 10.11%). The mean grain size ranged from 66.67 μm to 129.68 μm, and became coarser in the upper 8.5 cm. Sediments distinctly coarsened in 1968, 1986, 2000, and 2011, whereas they suddenly became finer at points during 1964, 1973, 1994, and 2013, displaying 10- and 20-year cycles (Fig.5). Core DH4-2 was taken from the maximum water depth of 70.6 m. Sediment variations in core DH4-2 were not consistent with core DH4-1 even though they were adjacent to each other. The bottom 4 cm sediment was characterized by a large mean particle size (mean: 101.18 μm) with a high sand content (64.48%). Grain sizes sharply decreased and sediment sorting decreased in 1952. Sediment parameters became more fluctuant during 1952–1979. Sediment grain size further reduced from 1979 until an increase in 2000. From 1952 to 1979, grain size parameters showed significant periodic fluctuations.

Cores L2 and L3 were collected from the Zhejiang coast at water depths of 35 m and 60 m, respectively. Sediment grain size changed most dramatically in these two cores. Core L2 was mainly composed of silt (mean: 79.88%) with two fining-coarsening cycles in relation to sediment grain size (Fig.5). In addition to the surface 1 cm and bottom 7 cm, the grain size of the core increased upwards. According to mean grain size, core L3 could be divided into four stages. The grain size remained stable at stage I (29–20 cm, period of 1977–1988) and then gradually increased from stage II (20–11 cm, period of 1988–2001) to III (11–7 cm, period of 2001–2006). In the top 6.5 cm of the core, mean grain size suddenly decreased and showed a continuous decreasing trend classified as stage IV (2007–2015). Standard deviation and skewness had the same distribution tendency while the kurtosis was inverse.

4.2.2 Sediment cores from the southern continental shelf

Cores DH8-1 and DH8-2 were located in the southern ECSIS and were dominated by silt. Core DH8-2 was more variable than core DH8-1, although it was collected from a deeper water depth. Unlike DH3-2, silt was dominant in the sediments of core DH8-1 even though they were collected at almost the same water depth (Fig.6). From 1987, sediment sorting became markedly worse and skewness showed a decreasing trend. The mean grain size showed a fluctuated increase in core DH8-1. From the bottom to the top, clay content was relatively uniform while the sand content gradually increased. In core DH8-2, changes in sand content were the main controlling factor of grain size variation. Average value of mean grain size sharply increased accompanied by a higher sand content from 1988. At the same time, sediment sorting decreased and skewness was more positively skewed. Sand content distinctly increased from 1987 both in core DH8-1 and core DH8-2. However, sand

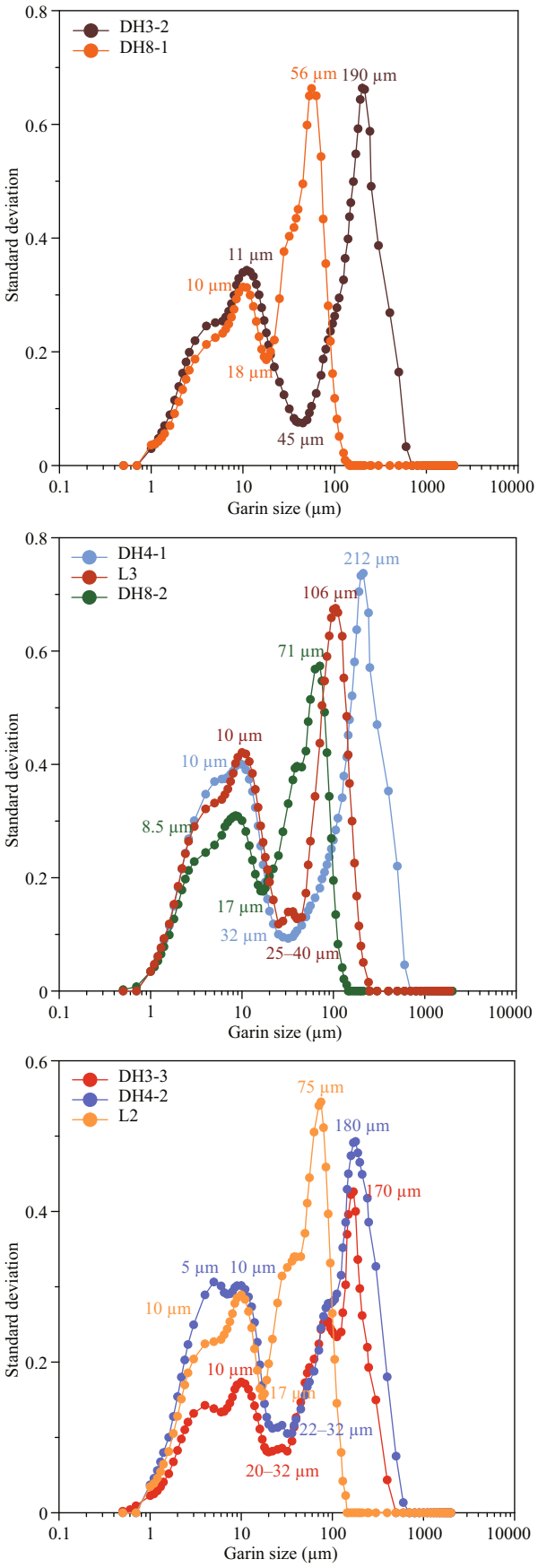

Fig.7 Grade-standard deviation curves of sediment cores

content in core DH8-1 fluctuated greatly while it remained relatively stable in core DH8-2 after 1987.

Variations in grain size differed among the cores. Mean grain size and standard deviation had opposite distribution characteristics while skewness and kurtosis varied synchronously in cores DH3-2, DH3-3, DH4-1, and DH4-2. In cores L2, DH8-1, and DH8-2, both mean grain size and standard deviation had similar distribution characteristics, and skewness and kurtosis varied synchronously. Whereas in core L3, both mean grain size and standard deviation roughly had same distribution characteristics, but skewness and kurtosis varied inconsistently.

4.2.3 Sensitive particle size components of the sediment cores

Sensitive particle size components of sediment cores were separated by the method of "grain size vs. standard deviation" selected by many previous researcher (Boulay et al., 2003; Sun et al., 2003; Xiang et al., 2005; Xiao and Li, 2005). As shown in Fig.7, the grain size vs. standard deviation value classes in each sediment core had two main peaks. These two classes represent populations of grains with the highest variability through time. Therefore, they are sensitive to different sedimentary environments. The sediment from the valley value was separated into two parts and the fine population was considered sensitive to the coastal current. Figures 3 and 7 show that the locations or grain sizes of breaking points of the two populations varied among cores depending on water depth and distance from the Changjiang River estuary. The only exception was core DH3-2 because it located outside Hangzhou Bay and therefore exposed to a stronger hydrodynamic force. The fine-grained population was relatively stable ranging from 8.5 μm to 11 μm with an average of 9.93 μm. However, the coarse-grain population significantly fluctuated from 56 μm to 212 μm with an average of 123.6 μm (Table 2). To some extent, both fine- and coarse-grain populations were related to water depth, such as in core L2, and source distance, for example in cores DH8-1 and DH8-2.

5 DISCUSSION

5.1 Changes in the Changjiang River sediment load

In recent decades, dam construction and irrigation have led to dramatic reductions in sediment discharge from many major rivers globally such as the Ebro River, Mississippi River, Nile River, and Changjiang

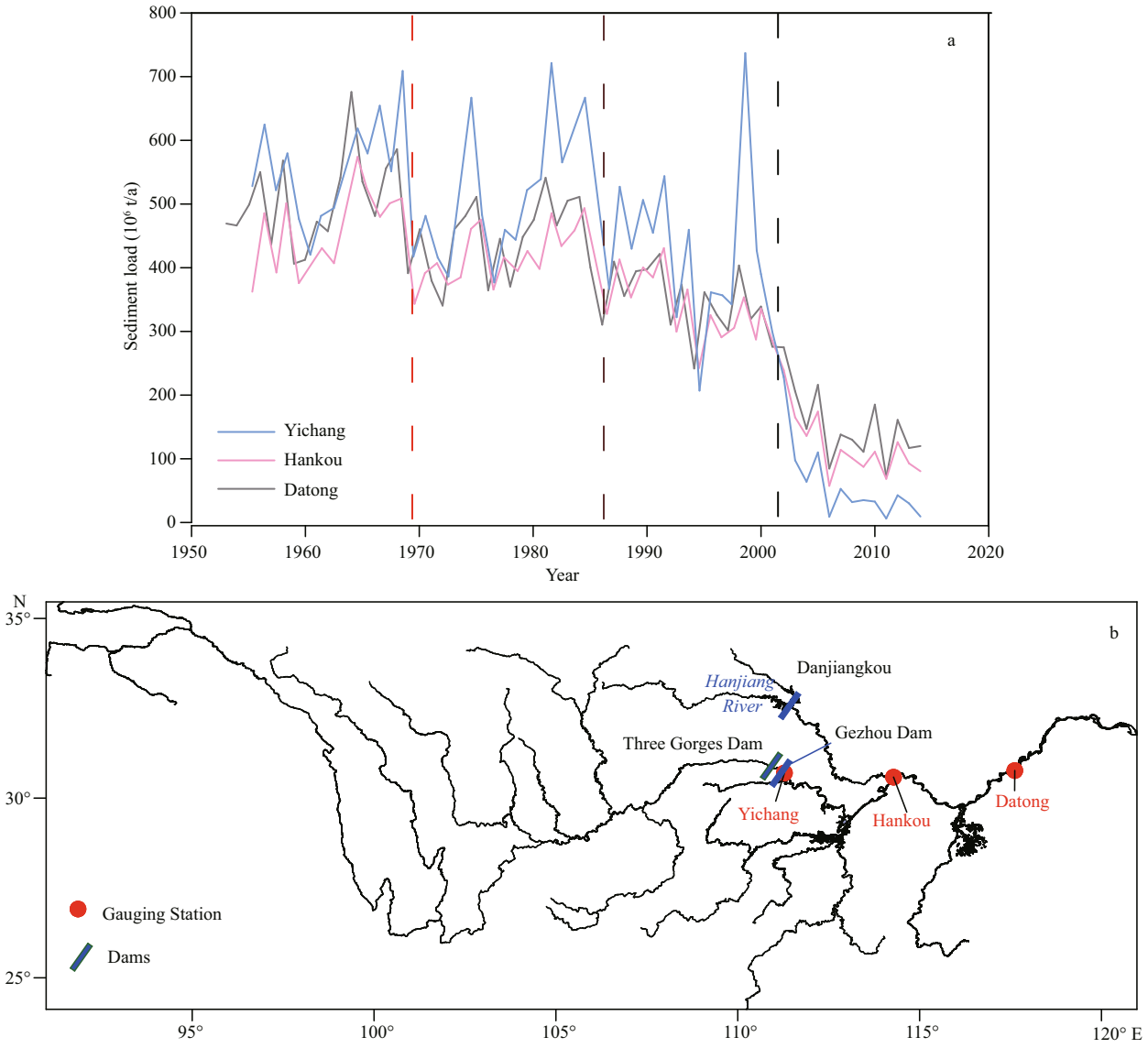

Fig.8 Sediment loads (in 10^6 t/a) at Yichang, Hankou, and Datong (a) and Changjiang River watershed (b), showing locations of the Three Gorges Dam (TGD) and the Yichang, Hankou, and Datong gauging stations

Table 2 Relationship between breaking points and grain size population according to water depth and core localities

Sample code	Water depth (m)	Breaking point (μm)	Fine population mode (μm)	Coarse population mode (μm)
DH3-2	52	45	11	190
DH3-3	59	20–32	10	170
DH4-1	61	32	10	212
DH4-2	70.6	22–32	10	180
L2	35	17	10	75
L3	60	25–40	10	106
DH8-1	51	18	10	56
DH8-2	61	17	8.5	71

River (Guillén and Palanques, 1997; Vörösmarty et al., 2003a; Nilsson et al., 2005; Syvitski et al., 2005; Walling, 2006; Blum and Roberts, 2009; Meade and Moody, 2010; Syvitski, 2011; Wang et al., 2011; Yang et al., 2011). Sediment load changes in the Changjiang River over recent decades have been observed. Since the 1950s, more than 50 000 dams have been built throughout the Changjiang River watershed (Yang et al., 2005; Xu et al., 2008) including the world's current largest dam, the TGD. Data from Datong gauging station showed that the mean annual sediment load has decreased in three reduction phases between 1951 and 2014 (Fig.8). It decreased from 490 Mt/a between 1951 and 1968 to 440 Mt/a over the following 17 years (1969–1985), followed by a 17-year interval

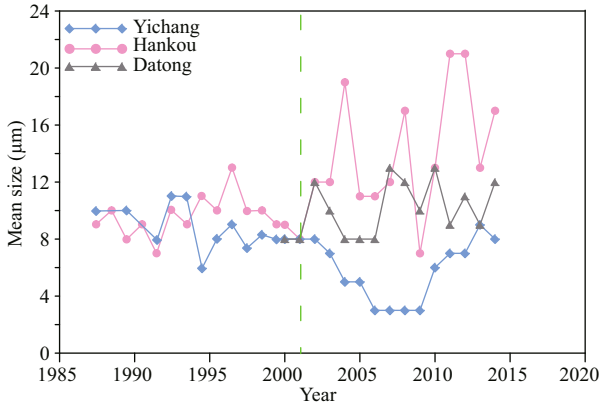

Fig.9 Mean grain size of suspended sediment at Yichang, Hankou and Datong (modified after Yang et al., 2011)

Table 3 Sediment loads (in 10^6 t/a) at Yichang, Hankou, and Datong

Station	Annual sediment load (10^6 t/a)			
	1950–1968	1969–1985	1986–2002	2003–2014
Yichang	540	520	410	43
Hankou	450	420	350	110
Datong	490	440	340	141

(1986–2002) with 340 Mt/a sediment load, and dramatically decreased to 141 Mt/a in 2003–2014 (data obtained from Changjiang River Water Conservancy Committee, Ministry of Water Conservancy of China).

Grain size variations in sediment cores on the ECSIS coincided with variations in river sediment load. Grain size increased upwards in most cores except core DH3-3. In cores DH4-1, L2 and DH8-2, grains were relatively coarse with a higher sand content before 1969. From 1969 to 1986, sand content and mean grain size decreased in half of the stations (DH4-1, L2, L3, and DH8-2) corresponding well to the first sediment load decrease stage in the Changjiang River. There were differences between the actual deposition rate and the constant deposition rate assumed by radioactive dating, thereby leading to 1–2 years deviation in some sediment cores. Yang et al. (2006) highlighted that this reduction phase was mainly caused by the activation of the reservoir on the Hanjiang River tributary since discharges at Yichang showed no distinct decreasing trend, while it was reduced in Hankou and Datong during this period (Fig.8). Due to the reduction in coarse sediments transported by the Changjiang River, particle size reduced on the inner shelf in this stage.

Between 1987 and 2002, sediment load decreased by 31% in Datong compared with 1950–1968 due to the construction of numerous dams and reservoirs as well as a water-soil conservation plan within the drainage basin (Yang et al., 2006) (Fig.8). Following the implementation of the TGD operation, sediment load drastically reduced to 141 Mt/a during 2003–2014 at Datong gauging station. Decreasing sediment load has made the Changjiang River channel change from an accretion state to an erosion state (Yang et al., 2011). The particle size of suspended sediment gradually increased at Hankou after 1986 and became far larger than that in Yichang after the closure of the TGD (Fig.9). This phenomenon suggests erosion of the river channel. A gradual increase in the amount of sand transport in Yichang, Hankou, and Datong during 2003–2014 has also supported this view. In sediment cores from shallow water less than 60 m (cores DH3-2, L2, and L3), the sand content gradually increased, and the mean grain size increase from 1987 and further increased after 2003. In general, the Changjiang River channel has converted from deposition to erosion in the late 1980s and strengthened after closure of the TGD in 2003 leading to an increase in sediment grain size discharging into the sea. In addition, the accretion/erosion balance in the subaqueous delta also been altered due to sediment starvation, which also contributed to the sediment coarsening. Correspondingly, sediments deposited in the ECSIS became coarser after 1987 and have further coarsened since 2003.

In deeper water (approximately 60 m water depth), the impact of modern terrigenous materials was relatively weak in cores DH3-3 and DH 4-2. These two cores were located in the CPFs area. CPFs refer to direct and large distance frontal intrusions from mean fronts of oceanic properties such as temperature, salinity, and chlorophyll-*a* concentration, with penetrating distances usually exceeding 50 km (He et al., 2010). The CPFs in the East China Sea can transport fine-grained sediments across the shelf to the east of 124°40′E or even further (Zhang et al., 2016). The strengthened variations in the CPFs may have changed the sedimentation patterns in cores DH3-3 and DH4-2. Therefore, there were no significant changes during the above three reduction periods in these two cores. The smaller grain size in the upper part of cores DH3-3 and DH4-2 may be due to the enhancement of the CPFs in the ECSIS. Variations between cores DH3-3 and DH4-2 may have also been caused by the cross-shelf penetrating front due to their different locations.

5.2 Impacts of the EAM on sedimentation

The ZFCC direction varies seasonally, it flows northward in summer due to the southeast monsoon and turns southward in winter when the northerly wind prevails (Fig.1). Sediments in the mud wedge along the entire ECSIS are mainly derived from the Changjiang River suspension transported by the coastal current in winter. Strong East Asian winter monsoon will accelerate the flow of ZFCC in winter and, accordingly, the sediment will become coarser, and vice versa. Previous studies considered that a fine-grained sediment population is transported by the ZFCC in winter (Xiao et al., 2006; Zhou et al., 2014). A fine-grained population reflects a much finer-grained material supply and a relatively gentle delivery force, such as an alongshore current, whereas a coarse-grained population indicates a less fine-grained matter supply and strong transporting hydrodynamic force, such as storm waves. Therefore, variations in the East Asia Winter Monsoon strengthening have obviously affected the mean grain size of the fine-grained population in the ECSIS sediments.

Therefore, it is more suitable to use a fine-grained population to reconstruct alongshore current and winter monsoon histories. The recalculated mean grain size of the fine-grained sensitive component was compared with strong breeze days (level 6 of the Beaufort wind scale, the speed of which is between 10.8–13.8 m/s) in winter (December, January, and February) monitored at Shengsi Island, in the Siberian High, and by EAWM indexes. Sediment grain sizes in cores showed consistent changes with these climate indexes (Fig.10). According to the strength of the EAWM, the time series can be separated into three stages during 1950–1987. Stage 1 comprised 1950 to 1964 in which the EAWM was stronger and the mean grain size of fine population was larger. After 1964, the EAWM became weaker until 1974, comprising stage 2, and correspondingly the sediments were relatively finer than stage 1. Stage 3 was the second strong EAWM period with coarser sediments in most sediment cores. From 1987 there was an obvious reduction in EAWM strength. Only cores DH3-2, DH3-3, DH4-1, and L2 recorded this reduction since this information may have been covered by other signals in the remaining sediment cores. Strong breeze days in Shengsi Island increased from 2001 and the mean grain size of the fine-grained population in cores DH3-3, DH4-1, DH4-2, and L3 increased correspondingly. This indicates that the coastal current strengthened and influenced sediment grain size, except the Changjiang River sediments, which were coarser.

5.3 Records of extreme events in sediments

Sediment grain size in the ECSIS is controlled by the alongshore current strength and the sediment source. Previous studies indicated that a fine-grained population reflects changes in the coastal current. Significant mutations in a coarse-grained population and other characteristics are beyond the threshold value of the variations in coastal currents. Usually, environmental factors that can lead to such drastic changes in hydrodynamic conditions and material supply are likely to be extreme events such as floods, typhoons, and storm surges. The research area is characterized by a high deposition rate with frequent typhoon and flood impacts. Sedimentary processes of typhoons and floods of the Changjiang River are likely to be recorded in this area. Since 1945, approximately 13 major floods occurred in the Changjiang River valley. Choosing Datong gauging station as the control point, the maximum peak runoff was two to three times the annual average (Changjiang River Water Conservancy Committee, Ministry of Water Conservancy of China). The increased runoff and flow velocity have led to an increase in coarse-grained components in the river sediments. Typhoons are extreme events that occur frequently in the East China Sea. When a typhoon occurs, seabed sediments resuspended due to enhanced hydrodynamics, and the fine particles are removed, leaving behind coarse particles. In the present study, the influences of typhoons on the inner shelf area are discussed based on the level 10 wind scope (Beaufort wind scale).

In the flood event layer, there were inverse graded and graded beddings that gradually transformed with both upper and lower layers due to the long duration of floods. In contrast, typhoons usually last a relatively short time. Sediments suddenly become coarser due to the sudden increase in hydrodynamic force. With the passage of the typhoon, the hydrodynamic force gradually weakens to normal levels with the deposited sediments became gradually finer.

Sediment grain size vertical variations were compared with typhoon and flood events based on extreme event deposition layer characteristics described above (Fig.11). Due to the difference between the actual deposition rate and the calculated deposition rate, sedimentary records of extreme events may have 1–2 years of error. Sediment cores DH3-2 and DH3-3, located closest to the Changjiang

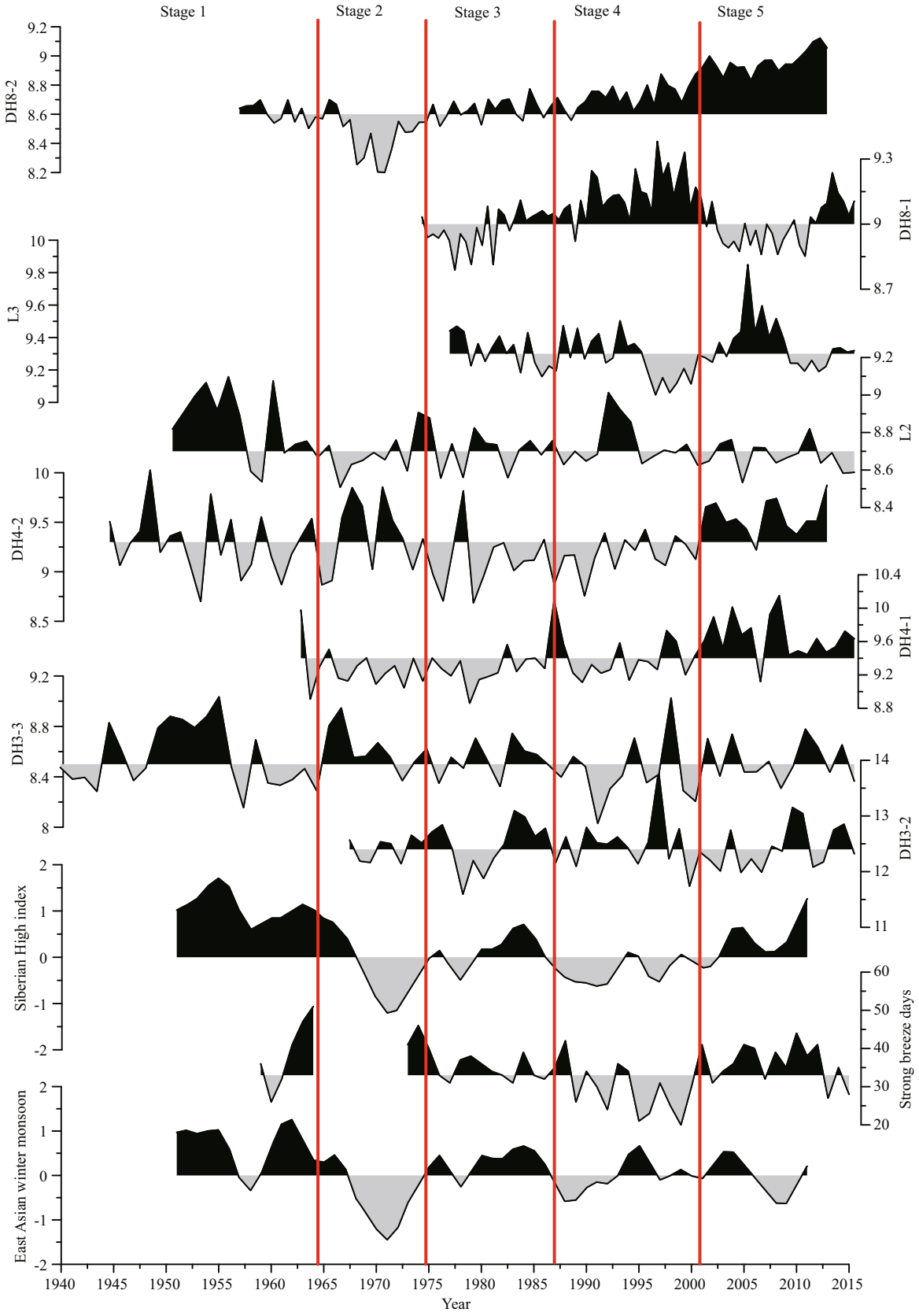

Fig.10 Relationships between mean grain size of the fine population in sediment cores and indicators of East Asian Winter Monsoon

Index data are obtained from the National Climate Center, China Meteorological Administration; strong breeze (>38.9 km/h) days were monitored in Shengsi Island (data were missing from 1965 to 1972).

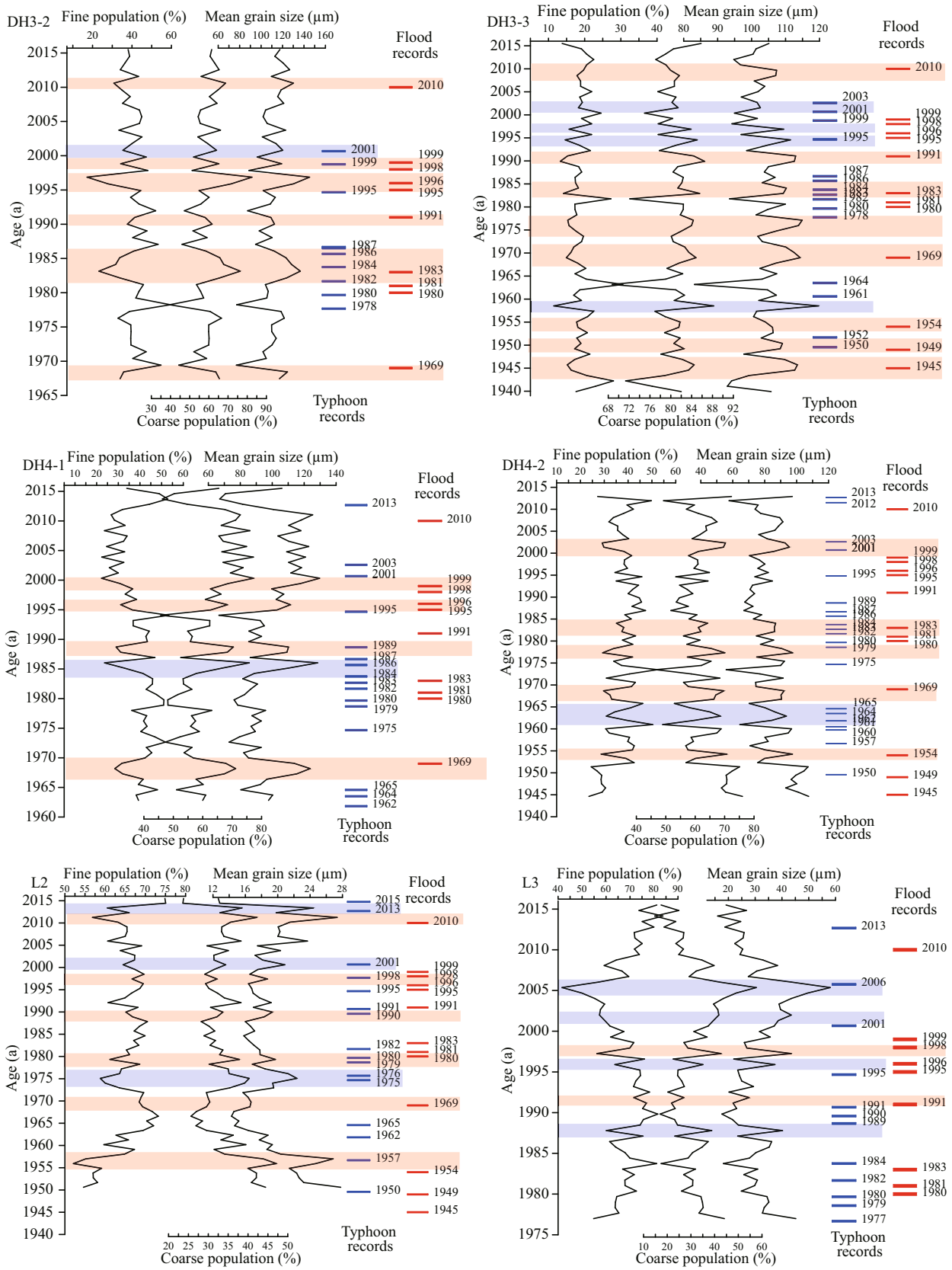

Fig.11 Vertical profiles of sediment particles in sediment cores with extreme events

Typhoon data are obtained from tcdata.typhoon.gov.cn (Ying et al., 2014); flood records are obtained from Shi et al. (2004).

To be continued

Fig.11 Continued

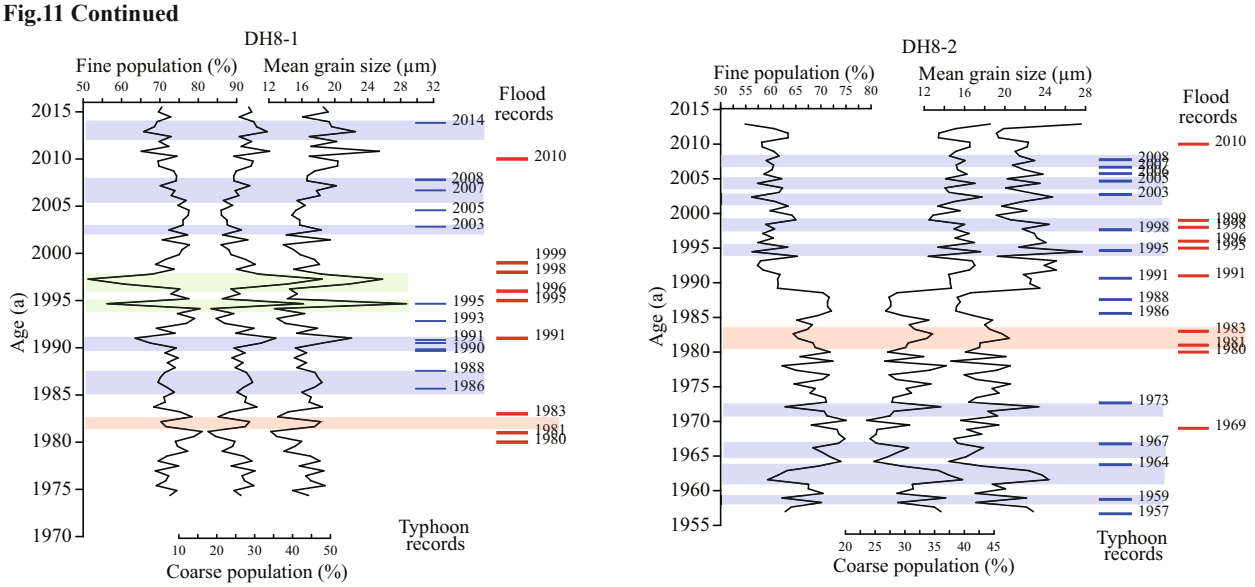

River mouth, have the most comprehensive record of Changjiang River flooding. To the south, some of the floods were not reflected in cores DH4-1 and DH4-2. The major floods of 1954 and 1998 were reflected in these four sediment cores by an increase in the coarse-grained population. Further south, with the exception of the shallowest core L2, floods were rarely recorded in three other cores. Typhoon records differed from floods. They were mainly reflected in the most southern cores DH8-1 and DH8-2. This phenomenon is related to the frequency of typhoons in different regions. The frequency of typhoons recorded in different sediment cores is consistent with the frequency of typhoon occurrence measured by Tian (2015): a high frequency in the southeast and reduced frequency to the northwest.

In core DH8-1, which was located in a Fujian coastal area, there were two distinct sediment coarsening events during the period 1990–2000. This showed a large amplitude that did not correspond well to typhoons or major Changjiang River floods. The categories of typhoons that passed through this region in 1995 and 1993 were 3–5. Whether they are strong enough to cause such a large amplitude or there were other factors in existence requires further study.

In summary, Changjiang River flooding mainly affects the northern area close to the estuary. Core L2 in a shallow water depth in the northern part of Zhejiang coast also had a good flood record. Other parts of the Zhejiang-Fujian coast did not significantly record Changjiang River flooding. However, typhoons had a greater impact on the southern part of the ECSIS where they frequently occur.

5.4 Effects of ENSO and solar activity on sedimentation

ENSO is an abnormal phenomenon in the air-sea interaction that has an important influence on global temperature and precipitation. It is closely related to the occurrence of floods and droughts in China (e.g., El Niño caused the Changjiang River basin to flood in 1998), and further influences material transport and deposition in the East China Sea (Jiang et al., 2006; Yu et al., 2009). To improve our understanding of the sedimentary process, the mean grain size time series of samples was determined in a spectral analysis. Mean grain size of all the sediment cores except core DH8-2 showed a 3–8-year periodic oscillation (Fig.12), which is consistent with the periodicity of ENSO. This period was more pronounced in the northern and near shore areas coinciding with changes in the magnitude of flooding impacts.

Periodic changes in solar activity can cause redistribution of the Earth's atmospheric energy, which greatly affects the global climate. Variations in sunspot and global sea surface temperature are in good agreement (Su and Yuan, 2005). Xiao et al. (2006) showed that a lower sunspot number corresponded to coarser sediments in the ECSIS mud. These authors suggested that reductions in solar irradiance may be caused an increasing temperature difference between continents and oceans during winter time, and resulted in a strengthening of the EAWM. Short-range solar activity has an 11-a significant sunspot period (Schwabe cycle) and a 22-a magnetic period (Hale cycle). The consistency of

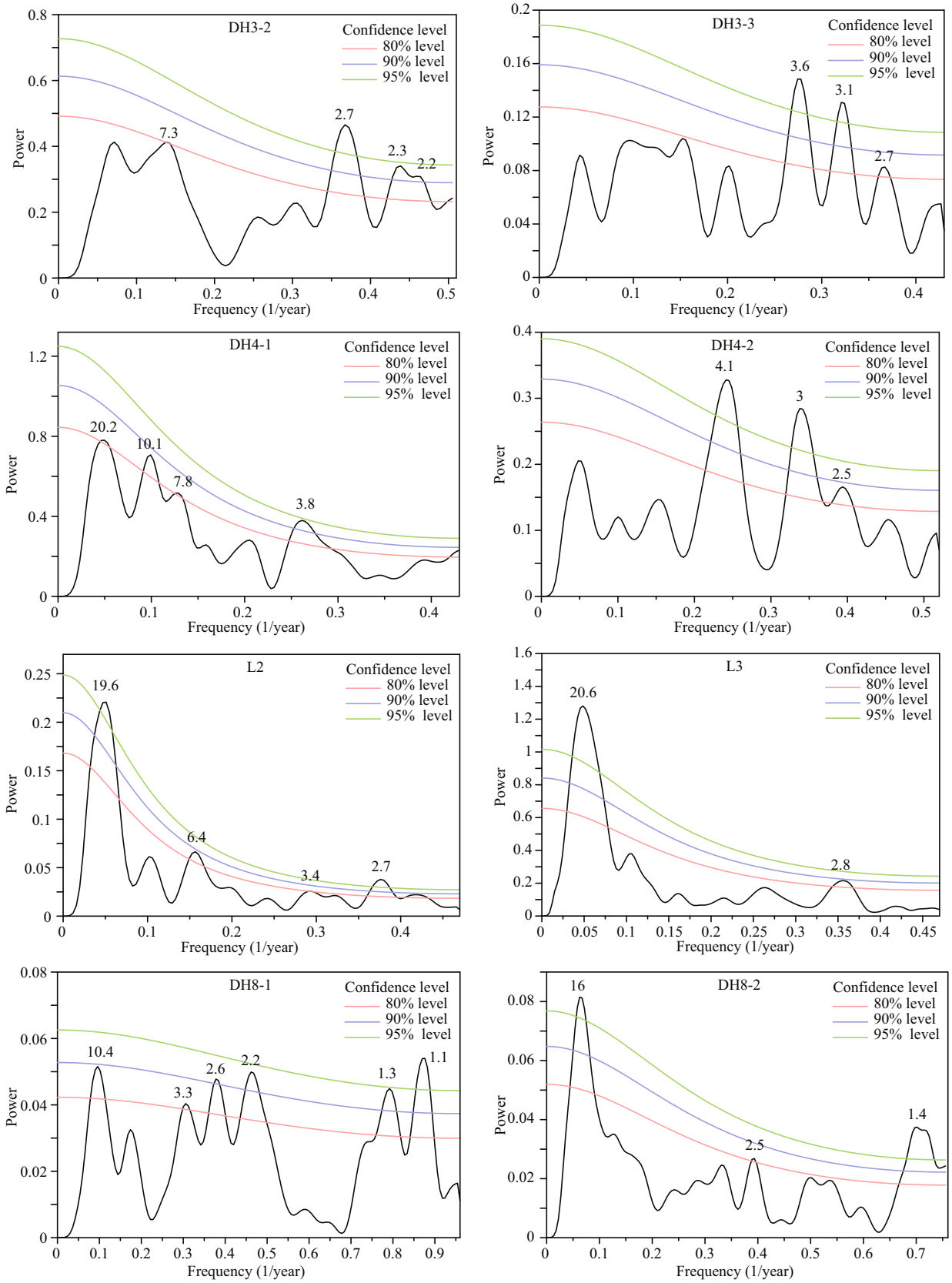

Fig.12 Frequency analyses of sediment cores mean grain size record for the entire samples

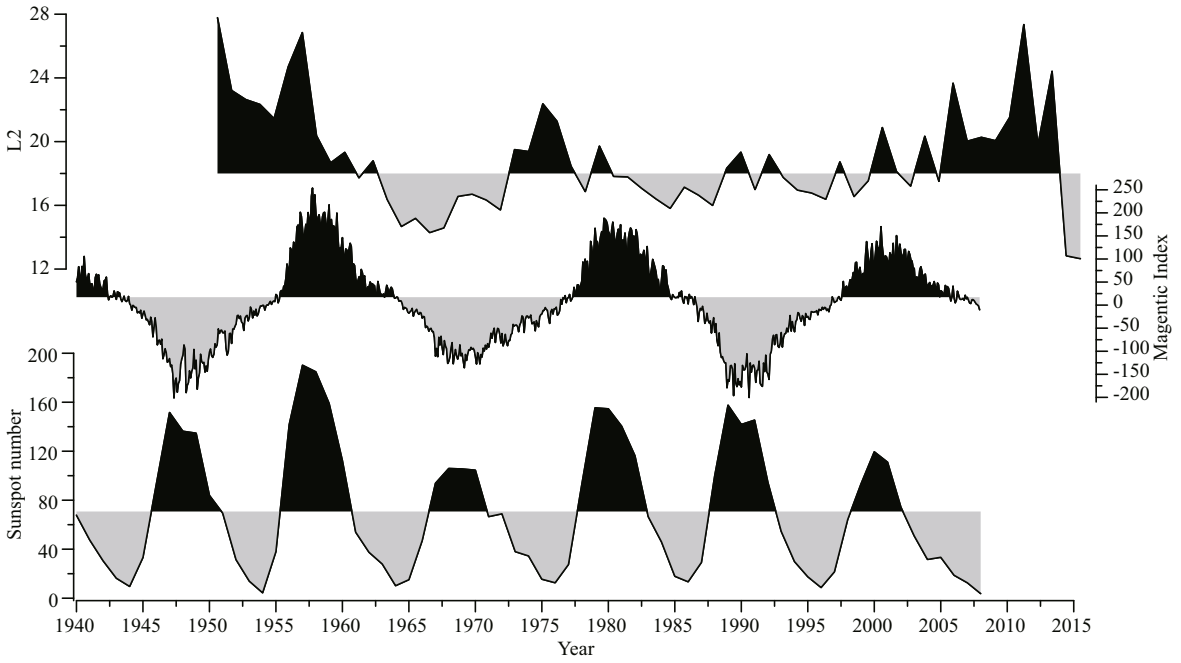

Fig.13 Temporal variations of mean grain size of core L2 and solar activity indices

Solar activity indices are obtained from Qu et al., 2008.

variations in mean grain size and solar activity indices (Fig.13) indicates that the statistically significant periodicities centering on 10–11 and 20–22 years in cores DH4-1, L2, L3, and DH8-1 (Fig.12) were caused by solar activity. Furthermore, the abrupt increases in silt and clay also displayed 10- and 20-year cycles in cores DH3-2 and DH4-1 (Fig.5). This may be due to the magnitude of CPF changes caused by solar activity.

In addition, the 16-year period of core DH8-2 may be caused by the superposition of other factors and solar activity variations. Both cores DH8-1 and DH8-2 showed significant periodicity centered on 1–2 a, potentially corresponding to the interannual oscillation of the EAM (Fig.12).

6 CONCLUSION

1) Sediments in the ECSIS reflect reductions in Changjiang River sediment load caused by human activities (especially dam constructions) since the 1950s. Due to the erosion of the Changjiang River channel and subaqueous delta, sediments deposited in the ECSIS became coarser after 1987 and further coarsened after 2003.

2) The EAM influenced the deposition process in the ECSIS by changing the intensity of the coastal currents. Mean grain size of the fine-grained population corresponded well to the strength of the EAWM. Parts of the sediment cores recorded the weakening of the EAWM after 1987.

3) The effects of river floods and typhoons in the ECSIS are limited in scope. Changjiang River flooding mainly impacts the northern shelf and the shallow area, while few records of Changjiang River floods were found in the southern shelf. In contrast, typhoons frequently occurred in the southern inner shelf and were markedly reflected in the sediment cores.

4) Mean grain size time series of sediment cores show statistical periodicities of 3–8, 10–11, and 20–22 years, corresponding to the periodicity of the ENSO and solar activity (Schwabe cycle and Hale cycle), respectively.

5) The ECSIS has a complicated sedimentary environment due to variations in influencing factors. Depositional processes are dominated by distinct factors in different locations. Therefore, environmental signals in sediment cores are a superimposition of multiple elements and the responses of each sediment core to every influencing factor are heterogenous. In general, changes in the Changjiang River debouched sediment load, grain size, and hydrodynamic force, which act as sediment delivery and erosion, are the main controlling factors in the ECSIS. ENSO and solar activity promoted these factors by affecting the monsoon, and dominating factors in multiyear and decade variation cycles of sedimentation.

7 DATA AVAILABILITY STATEMENT

1) The sediment loads and mean grain size of suspended sediment dataset of Changjiang River gauging stations during the current study are available from the published article "50 000 dams later: Erosion of the Changjiang River and its delta" and the Changjiang River Water Conservancy Committee, Ministry of Water Conservancy of China (http://www.cjh.com.cn/pages/nsgb.html).

2) The Siberian High index and East Asian Winter Monsoon dataset are available from the National Climate Center, China Meteorological Administration (http://cmdp.ncc.cma.gov.cn/cn/index.htm).

3) Strong breeze data in Shengsi Island are available from website: http://en.tutiempo.net/.

4) Typhoon data are available from the China Meteorological Administration tropical cyclone database. (http://www.tcdata.typhoon.gov.cn).

5) Floods data are included in the published article "Preliminary analysis on the relation between the evolution of heavy floods in the Changjiang River catchment and the climate changes since 1840" and the Changjiang River Water Conservancy Committee, Ministry of Water Conservancy of China. (http://www.cjh.com.cn/pages/nsgb.html).

6) Solar activity indices are obtained from the published article "The time sequence of the magnetic index of the sunspot magnetic field".

8 ACKNOWLEDGEMENT

We thank chief editor Roger Z. YU for the editorial handling of the manuscript and two reviewers for their valuable comments. We thank all of the investigators for their help in collecting samples.

References

Allen M R, Ingram W J. 2002. Constraints on future changes in climate and the hydrologic cycle. *Nature*, **419**(6903): 224-232, https://doi.org/10.1038/nature01092.

Blum M D, Roberts H H. 2009. Drowning of the Mississippi Delta due to insufficient sediment supply and global sea-level rise. *Nature Geoscience*, **2**(7): 488-491, https://doi.org/10.1038/ngeo553.

Boulay S, Colin C, Trentesaux A et al. 2003. Mineralogy and sedimentology of pleistocene sediment in the South China Sea (ODP Site 1144). *In*: Prell W L, Wang P, Blum P et al eds. Proceedings of the Ocean Drilling Program Scientific Results. p.1-21.

Carriquiry J D, Sánchez A. 1999. Sedimentation in the Colorado River delta and Upper Gulf of California after nearly a century of discharge loss. *Marine Geology*, **158**(1-4): 125-145, https://doi.org/10.1016/S0025-3227(98)00189-3.

DeMaster D J, McKee B A, Nittrouer C A et al. 1985. Rates of sediment accumulation and particle reworking based on radiochemical measurements from continental shelf deposits in the East China Sea. *Continental Shelf Research*, **4**(1-2): 143-158, https://doi.org/10.1016/0278-4343(85)90026-3.

Easterling D R, Meehl G A, Parmesan C et al. 2000. Climate extremes: observations, modeling, and impacts. *Science*, **289**(5487): 2 068-2 074, https://doi.org/10.1126/science.289.5487.2068.

Guillén J, Palanques A. 1997. A historical perspective of the morphological evolution in the lower Ebro river. *Environmental Geology*, **30**(3-4): 174-180, https://doi.org/10.1007/s002540050144.

Guo Z G, Yang Z S, Fan D J et al. 2003. Seasonal variation of sedimentation in the Changjiang Estuary mud area. *Journal of Geographical Sciences*, **13**(3): 348-354, https://doi.org/10.1007/BF02837510.

Gupta H, Kao S J, Dai M H. 2012. The role of mega dams in reducing sediment fluxes: a case study of large Asian rivers. *Journal of Hydrology*, **464-465**: 447-458, https://doi.org/10.1016/j.jhydrol.2012.07.038.

He L, Li Y, Zhou H et al. 2010. Variability of cross-shelf penetrating fronts in the East China Sea. *Deep Sea Research Part II*: *Topical Studies in Oceanography*, **57**(19-20): 1 820-1 826, https://doi.org/10.1016/j.dsr2.2010.04.008.

Hu B Q, Yang Z S, Zhao M X et al. 2012. Grain size records reveal variability of the East Asian Winter Monsoon since the Middle Holocene in the Central Yellow Sea mud area, China. *Science China Earth Sciences*, **55**(10): 1 656-1 668, https://doi.org/10.1007/s11430-012-4447-7.

Jiang T, Zhang Q, Zhu D M et al. 2006. Yangtze floods and droughts (China) and teleconnections with ENSO activities (1470-2003). *Quaternary International*, **144**(1): 29-37, https://doi.org/10.1016/j.quaint.2005.05.010.

Labat D, Goddéris Y, Probst J L et al. 2004. Evidence for global runoff increase related to climate warming. *Advances in Water Resources*, **27**(6): 631-642, https://doi.org/10.1016/j.advwatres.2004.02.020.

Li J B. 2008. Regional Geology of East China Sea. China Ocean Press, Beijing, China. p.4. (in Chinese)

Li Q F, Yu M X, Lu G B et al. 2011. Impacts of the Gezhouba and Three Gorges reservoirs on the sediment regime in the Yangtze River, China. *Journal of Hydrology*, **403**(3-4): 224-233, https://doi.org/10.1016/j.jhydrol.2011.03.043.

Lim D I, Choi J Y, Jung H S et al. 2007. Recent sediment accumulation and origin of shelf mud deposits in the Yellow and East China Seas. *Progress in Oceanography*, **73**(2): 145-159, https://doi.org/10.1016/j.pocean.2007.02.004.

Liu F, Chen S L, Dong P et al. 2012. Spatial and temporal variability of water discharge in the Yellow River Basin over the past 60 years. *Journal of Geographical Sciences*, **22**(6): 1 013-1 033, https://doi.org/10.1007/s11442-012-0980-8.

Liu J P, Li A C, Xu K H et al. 2006. Sedimentary features of the Yangtze River-derived along-shelf clinoform deposit in

the East China Sea. *Continental Shelf Research*, **26**(17-18): 2 141-2 156, https://doi.org/10.1016/j.csr.2006.07.013.

Liu J P, Xu K H, Li A C et al. 2007. Flux and fate of Yangtze River sediment delivered to the East China Sea. *Geomorphology*, **85**(3-4): 208-224, https://doi.org/10.1016/j.geomorph.2006.03.023.

Liu M, Fan D J. 2011. Geochemical records in the subaqueous Yangtze River delta and their responses to human activities in the past 60 years. *Chinese Science Bulletin*, **56**(6): 552-561, https://doi.org/10.1007/s11434-010-4256-3.

Liu S D, Qiao L L, Li G X et al. 2015. Distribution and cross-front transport of suspended particulate matter over the inner shelf of the East China Sea. *Continental Shelf Research*, **107**: 92-102, https://doi.org/10.1016/j.csr.2015.07.013.

Liu S F, Shi X F, Liu Y G et al. 2011. Environmental record from the mud area on the inner continental shelf of the East China Sea since the mid-Holocene. *Acta Oceanologica Sinica*, **30**(4): 43-52, https://doi.org/10.1007/s13131-011-0132-5.

Liu Y, Zhai S K, Li J. 2010. Depositional records in the mud areas of Changjiang Estuary and off Min-Zhe coast and their influence factors. *Marine Geology & Quaternary Geology*, **30**(5): 1-10. (in Chinese with English abstract)

McManus J. 1988. Grain size determination and interpretation. *In*: Tucker M E ed. Techniques in Sedimentology. Blackwell Scientific, Oxford, England. p.63-85.

Meade R H, Moody J A. 2010. Causes for the decline of suspended-sediment discharge in the Mississippi River system, 1940-2007. *Hydrological Processes*, **24**(1): 35-49, https://doi.org/10.1002/hyp.7477.

Milliman J D, Farnsworth K L, Jones P D et al. 2008. Climatic and anthropogenic factors affecting river discharge to the global ocean, 1951-2000. *Global and Planetary Change*, **62**(3-4): 187-194, https://doi.org/10.1016/j.gloplacha.2008.03.001.

Milliman J D, Farnsworth K L. 2011. River Discharge to the Coastal Ocean: A Global Synthesis. Cambridge University Press, Cambridge. 383p. https://doi.org/10.1017/CBO9780511781247.

Milliman J D. 1997. Blessed dams or damned dams? *Nature*, **388**(6623): 325-326, https://doi.org/10.1038/386325a0.

Nilsson C, Reidy C A, Dynesius M et al. 2005. Fragmentation and flow regulation of the world's large river systems. *Science*, **308**(5720): 405-408, https://doi.org/10.1126/science.1107887.

Qu W Z, Qin T, Deng S G et al. 2008. The time sequence of the magnetic index of the sunspot magnetic field. *Progress in Geophysics*, **23**(6): 1 727-1 735. (in Chinese with English abstract)

Restrepo J C, Ortíz J C, Pierini J et al. 2014. Freshwater discharge into the Caribbean Sea from the rivers of Northwestern South America (Colombia): magnitude, variability and recent changes. *Journal of Hydrology*, **509**: 266-281, https://doi.org/10.1016/j.jhydrol.2013.11.045.

Schulz M, Mudelsee M. 2002. REDFIT: estimating red-noise spectra directly from unevenly spaced paleoclimatic time series. *Computers & Geosciences*, **28**(3): 421-426.

Shi Y F, Jiang T, Su B D et al. 2004. Preliminary analysis on the relation between the evolution of heavy floods in the Yangtze River catchment and the climate changes since 1840. *Journal of Lake Sciences*, **16**(4): 289-297, https://doi.org/10.18307/2004.0401. (in Chinese with English abstract)

Su J L , Yuan Y L. 2005. Hydrology in Chinese Offshore. China Ocean Press, Beijing, China. p.41. (in Chinese)

Sun Y B, Gao S, Li J. 2003. Preliminary analysis of grain-size populations with environmentally sensitive terrigenous components in marginal sea setting. *Chinese Science Bulletin*, **48**(2): 184-187, https://doi.org/10.1360/03tb9038.

Syvitski J P M, Milliman J D. 2007. Geology, geography, and humans battle for dominance over the delivery of fluvial sediment to the coastal ocean. *The Journal of Geology*, **115**(1): 1-19, https://doi.org/1-19.10.1086/509246.

Syvitski J P M, Vörösmarty C J, Kettner A J et al. 2005. Impact of humans on the flux of terrestrial sediment to the global coastal ocean. *Science*, **308**(5720): 376-380, https://doi.org/10.1126/science.1109454.

Syvitski J P M. 2011. Global sediment fluxes to the Earth's coastal ocean. *Applied Geochemistry*, **26**(Suppl 1): S373-S374, https://doi.org/10.1016/j.apgeochem.2011.03.064.

Tian Y. 2015. Recognition and Reconstruction of Event Deposits from the Mud Area in the Inner Shelf of the East China Sea in the Past 100 Years. Ocean University of China, Qingdao, China. p.19-21. (in Chinese with English abstract)

Vörösmarty C J, Bjerklie D M, Dingman S L et al. 2003a. River discharge strategies from space. *Geophysical Research Abstracts*, **5**: 11 300.

Vörösmarty C J, Meybeck M, Fekete B et al. 2003b. Anthropogenic sediment retention: major global impact from registered river impoundments. *Global and Planetary Change*, **39**(1-2): 169-190, https://doi.org/10.1016/S0921-8181(03)00023-7.

Walling D E. 2006. Human impact on land–ocean sediment transfer by the world's rivers. *Geomorphology*, **79**(3-4): 192-216, https://doi.org/10.1016/j.geomorph.2006.06.019.

Wang H J, Saito Y, Zhang Y et al. 2011. Recent changes of sediment flux to the western Pacific Ocean from major rivers in East and Southeast Asia. *Earth-Science Reviews*, **108**(1-2): 80-100, https://doi.org/10.1016/j.earscirev.2011.06.003.

Wang P X. 2009. Global monsoon in a geological perspective. *Chinese Science Bulletin*, **54**(7): 1 113-1 136, https://doi.org/10.1007/s11434-009-0169-4.

Xiang R, Yang Z S, Guo Z G et al. 2005. Paleoenvironmental implications of grain-size component variations in the mud area southwest off Cheju Island, ECS. *Earth Science-Journal of China University of Geosciences*, **30**(5): 582-588. (in Chinese with English abstract)

Xiao S B, Li A C, Liu J P et al. 2006. Coherence between solar activity and the East Asian winter monsoon variability in the past 8000 years from Yangtze River-derived mud in the East China Sea. *Palaeogeography*, *Palaeoclimatology*,

Palaeoecology, **237**(2-4): 293-304, https://doi.org/10.1016/j.palaeo.2005.12.003.

Xiao S B, Li A C. 2005. A study on environmentally sensitive grain-size population in inner shelf of the East China Sea. *Acta Sedimentologica Sinica*, **23**(1): 122-129. (in Chinese with English abstract)

Xu F J, Li A C, Li T G et al. 2011. The paleoenvironmental significance of magnetic susceptibility of sediments on the East China Sea inner shelf since the last deglaciation. *Acta Oceanologica Sinica*, **33**(1): 91-97. (in Chinese with English abstract)

Xu F J, Li A C, Xu K H et al. 2009a. Cold event at 5 500 a BP recorded in mud sediments on the inner shelf of the East China Sea. *Chinese Journal of Oceanology and Limnology*, **27**(4): 975-984, https://doi.org/10.1007/s00343-009-9273-1.

Xu K H, Li A C, Liu J P et al. 2012. Provenance, structure, and formation of the mud wedge along inner continental shelf of the East China Sea: a synthesis of the Yangtze dispersal system. *Marine Geology*, **291-294**: 176-191, https://doi.org/10.1016/j.margeo.2011.06.003.

Xu K H, Milliman J D, Li A C et al. 2009b. Yangtze-and Taiwan-derived sediments on the inner shelf of East China Sea. *Continental Shelf Research*, **29**(18): 2 240-2 256, https://doi.org/10.1016/j.csr.2009.08.017.

Xu K H, Milliman J D, Xu H. 2010. Temporal trend of precipitation and runoff in major Chinese Rivers since 1951. *Global and Planetary Change*, **73**(3-4): 219-232, https://doi.org/10.1016/j.gloplacha.2010.07.002.

Xu K H, Milliman J D, Yang Z S et al. 2006. Yangtze sediment decline partly from Three Gorges Dam. *EOS*, *Transactions American Geophysical Union*, **87**(19): 185-190, https://doi.org/10.1029/2006EO190001.

Xu K H, Milliman J D, Yang Z S et al. 2008. Climatic and anthropogenic impacts on water and sediment discharges from the Yangtze River (Changjiang), 1950-2005. *In*: Gupta A ed. Large Rivers: Geomorphology and Management. John Wiley & Sons. New York, America, p.609-626.

Yang S L, Gao A, Hotz H M et al. 2005. Trends in annual discharge from the Yangtze River to the sea (1865-2004). *Hydrological Sciences Journal*, **50**(5): 825-836, https://doi.org/10.1623/hysj.2005.50.5.825.

Yang S L, Milliman J D, Li P et al. 2011. 50,000 dams later: erosion of the Yangtze River and its delta. *Global and Planetary Change*, **75**(1-2): 14-20, https://doi.org/10.1016/j.gloplacha.2010.09.006.

Yang S L, Milliman J D, Xu K H et al. 2014. Downstream sedimentary and geomorphic impacts of the Three Gorges Dam on the Yangtze River. *Earth-Science Reviews*, **138**: 469-486, https://doi.org/10.1016/j.earscirev.2014.07.006.

Yang S L, Xu K H, Milliman J D et al. 2015. Decline of Yangtze River water and sediment discharge: impact from natural and anthropogenic changes. *Scientific Reports*, **5**: 12 581, https://doi.org/10.1038/srep12581.

Yang S L, Zhang J, Xu X J. 2007. Influence of the Three Gorges Dam on downstream delivery of sediment and its environmental implications, Yangtze River. *Geophysical Research Letters*, **34**(10): L10401, https://doi.org/10.1029/2007GL029472.

Yang Z S, Wang H J, Saito Y et al. 2006. Dam impacts on the Changjiang (Yangtze) River sediment discharge to the sea: the past 55 years and after the Three Gorges Dam. *Water Resources Research*, **42**(4): W04407, https://doi.org/10.1029/2005WR003970.

Ying M, Zhang W, Yu H et al. 2014. An overview of the China Meteorological Administration tropical cyclone database. *Journal of Atmospheric and Oceanic Technology*, **31**(2): 287-301, https://doi.org/10.1175/JTECH-D-12-00119.1.

Yu F L, Chen Z Y, Ren X Y et al. 2009. Analysis of historical floods on the Yangtze River, China: Characteristics and explanations. *Geomorphology*, **113**(3-4): 210-216, https://doi.org/10.1016/j.geomorph.2009.03.008.

Yuan D L, Hsueh Y. 2010a. Dynamics of the cross-shelf circulation in the Yellow and East China Seas in winter. *Deep Sea Research Part II*: *Topical Studies in Oceanography*, **57**(19): 1 745-1 761.

Yuan D L, Li Y, He L et al. 2010b. An observation of the three-dimensional structure of a cross-shelf penetrating front off the Changjiang mouth. *Deep Sea Research Part II Topical Studies in Oceanography*, **57**(19): 1 827-1 834.

Yuan D L, Qiao F L, Su J. 2005. Cross-shelf penetrating fronts off the southeast coast of China observed by MODIS. *Geophysical Research Letters*, **32**(19): 06.

Yuan D L, Zhu J R, Li C Y et al. 2008. Cross-shelf circulation in the Yellow and East China Seas indicated by MODIS satellite observations. *Journal of Marine Systems*, **70**(1): 134-149.

Zhang J C, Lin Z G. 1992. Climate of China. Shanghai Scientific and Technical Publishers,Shanghai, China. p.173-176. (in Chinese)

Zhang K D, Li A C, Dong J et al. 2016. Detrital mineral distributions in surface sediments of the East China Sea: implications for sediment provenance and sedimentary environment. *Acta Sedimentologica Sinica*, **34**(5): 902-911. (in Chinese with English abstract)

Zhang S R, Lu X X, Higgitt D L et al. 2008. Recent changes of water discharge and sediment load in the Zhujiang (Pearl River) Basin, China. *Global and Planetary Change*, **60**(3-4):365-380,https://doi.org/10.1016/j.gloplacha.2007.04.003.

Zhao Y F, Zou X Q, Gao J H et al. 2017. Recent sedimentary record of storms and floods within the estuarine-inner shelf region of the East China Sea. *The Holocene*, **27**(3): 439-449, https://doi.org/10.1177/0959683616660165.

Zhou X, Yang W Q, Xiang R et al. 2014. Re-examining the potential of using sensitive grain size of coastal muddy sediments as proxy of winter monsoon strength. *Quaternary International*, **333**: 173-178, https://doi.org/10.1016/j.quaint.2013.12.013.